Pergamon

Cement and Concrete Research, Vol. 28, No. 7, pp. 1071–1083, 1998

0008-8846/98 $19.00 + .00

PII S0008-8846(98)00060-X

DETECTION OF THE CORROSION DAMAGE IN REINFORCED CONCRETE MEMBERS BY ULTRASONIC TESTING

W. Yeih and R. Huang[1]
Department of Harbor and River Engineering, National Taiwan Ocean University,
Keelung, Taiwan, R.O.C.

(Received January 4, 1996; in final form April 21, 1998)

ABSTRACT

In this study, the amplitude attenuation method in ultrasonic testing was used to evaluate the corrosion damage of reinforced concrete members. It is found that the amplitude attenuation method has good performance in corrosion detection for reinforced concrete members. There exists a consistent relationship between the average amplitude attenuation and the electrochemical parameters such as open circuit potential values, the instantaneous corrosion rate, and thickness loss. *© 1998 Elsevier Science Ltd*

Introduction

Corrosion damage in structures subjected to a marine environment is a serious problem, and the early detection of corrosion damage can prevent possible loss of human life and property. Traditionally, electrochemical methods such as the open circuit potential (OCP) method, DC polarization method, and AC impedance method have been used for corrosion detection (1). All these methods were originally developed from simple experiments where metal was immersed in various environments, and uniform corrosion all over the specimen was assumed because the nature of such experiments allowed the whole metal surface to be in contact with the corrosive environment. Such electrochemical methods can only obtain overall information theoretically. However, pitting corrosion often occurs in reinforcing steel in reinforced-concrete (RC) members because the local environment surrounding the metal surface is not uniform, and inappropriate overloading in RC structures may induce cracks in concrete such that chloride ions from the environment can penetrate the concrete along cracks faster than other parts without cracks. Another method is the so-called double electrode half cell potential method (2), which can obtain equal potential contours for local evaluation of the corrosion damage. The double electrode half cell potential method can indicate the thermodynamic trend of the corrosion phenomenon, but can not quantitatively describe the corrosion rate. The electrochemical measurements for detection of corrosion damage in RC members may underestimate the local pitting corrosion rate because the electrochemical parameters represent global information obtained by taking an average of the total amount of local corrosion on the whole metal surface area.

[1]To whom correspondence should be addressed.

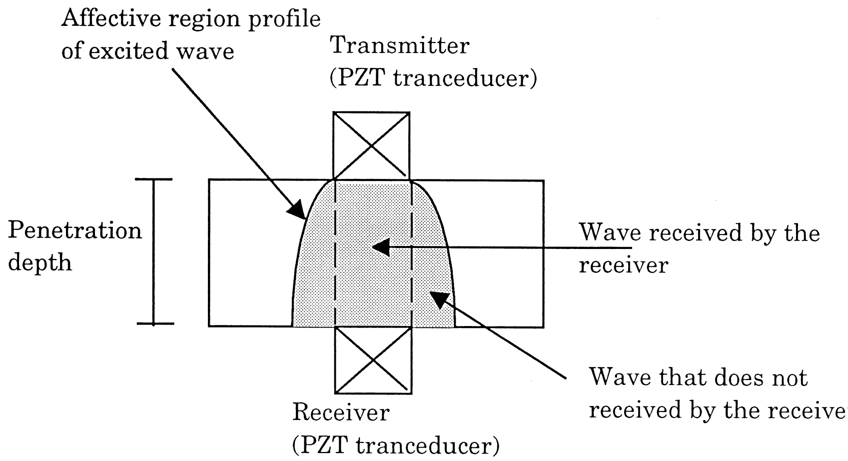

FIG. 1.
An illustration of the UT method.

Like the electrochemical methods, the ultrasonic testing (UT) method has been well developed and used for flaw detection in metal (3–9), but UT has not been used in concrete detection as commonly as it has been used in metal detection. The reason for the limited applications of UT in concrete structures is that the penetration depth required in concrete members is usually much longer than that in metal members. For full penetration of ultrasonic wave in RC members, a lower excitation frequency (e.g., 500 KHz) should be used. However, a lower excitation frequency induces longer wave length, so that a loss of resolution may occur. As shown in Figure 1, the UT method (direct pitch and catch method) employs an excited transducer (usually PZT is used) to excite a mechanical wave, and the mechanical wave propagates inside the object to be detected. A receiver (PZT) is mounted on the other side of the object to receive the signals of this mechanical wave. According to the wave signals, two important parameters, pulse velocity and amplitude, are frequently used to analyze the integrity of the object. The pulse velocity is calculated from dividing the total wave path length by the total flying time it required. When a flaw (for example, a major crack) is along the wave path, the total flying time of the wave is longer due to the diffraction of wave. The amplitude attenuation is mainly due to the dispersion and dissipation of wave. In a corroded RC structure, the scattering phenomenon of wave by cracks, the dissipating oscillation due to cracks, and reduction of transmitted wave due to the change of acoustic impedance either from cracks inside the concrete or rust on the concrete-rebar interface result in additional amplitude attenuation compared to an undamaged body. According to the UT method (10), the wave signals reflect information along the wave path. When only a spot is examined, this is called an A-scan. When spots are connected into a line, this is called a B-scan. When the lines of B-scan are combined, information on the examined surface can construct the C-scan. For a 3-D view, the D-scan can be constructed by combining information on all surfaces of the object. The above-mentioned scanning methods in UT are shown in Figure 2.

Although application of the UT method in concrete detection has been limited, there have been several successful attempts. Concrete strength was reported to have an empirical

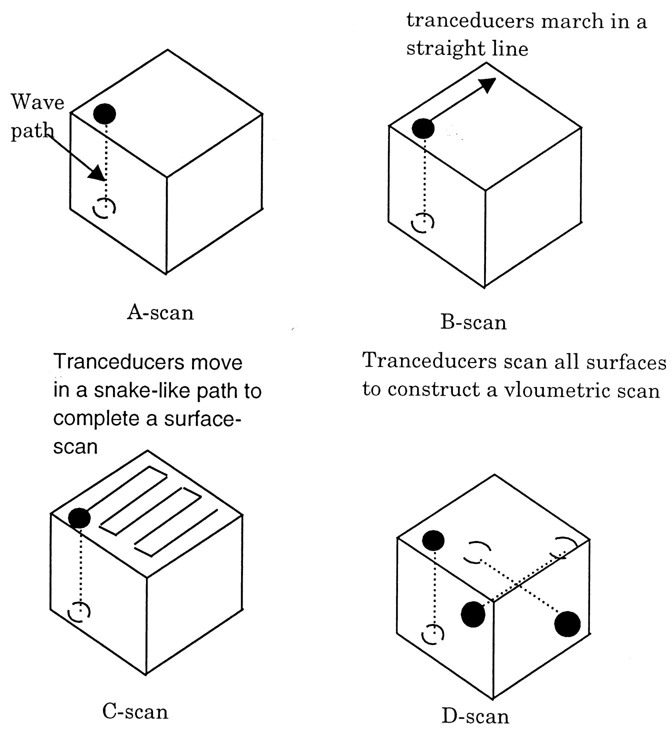

FIG. 2.
The A-scan, B-scan, C-scan, and D-scan in UT.

relationship with UT pulse velocity (11–12), and the pulse velocity method was used to evaluate cracks in concrete (13). The above-mentioned attempts were based on the pulse velocity method.

In this study, the UT amplitude attenuation method was used to evaluate corrosion damage in RC members. If the deterioration of the RC structure is mainly caused by corrosion, microcracks near the reinforcing steel or major cracks which have developed from the concrete-rebar interface and rust should cause amplitude attenuation (equivalently, energy loss). The amplitude attenuation has good correlation with the corrosion damage. Furthermore, the average UT amplitude attenuation and electrochemical parameters have a consistent relationship.

Experiment Procedure

The reinforcing steel used in this research was made of medium carbon steel, the chemical composition of which is listed in Table 1. Two sizes of rebars (#6 and #8 rebars) were used. Two concrete mixes were selected as shown in Table 2 To achieve a smooth concrete surface to ensure better contact with the PZT ultrasonic probe, a high slump was designed. The specimen was a block with dimensions of 30 × 30 × 10 cm, and the rebar was embedded in the concrete as shown in Figure 3 The length of the rebar embedded in the concrete was 22 cm, and part of the surface of the rebar was coated with epoxy. Electrical wires were

TABLE 1
The chemical composition of steel rebars.

Element	C	Cu	Si	P	S	Ni	Cr	Mo	Sn	Mn	Fe
weight %	0.36	0.23	0.2	0.04	0.03	0.11	0.12	0.01	0.02	0.61	bal.*

*bal. means balanced.

connected to the rebars to speed up the corrosion damage and electrochemical measurements. The specimens were labeled as 6A, 6B, 8A, and 8B, where the first digit represented the number of rebars and the letter represented the concrete designation. For each group, two specimens were prepared to check the consistency of the data. After demolding, the specimens were cured using the standard curing method for 28 days.

After curing, the specimens were immersed in 3.5% NaCl solution and connected to a DC power supply to accelerate the corrosion process. The rebar was arranged as an anode and titanium alloy mesh as a cathode. The constant current density, 1 mA/cm^2, was impressed according to previous studies. Once every 24 h, the impressed current was cut off, and the OCP values, DC polarization resistance values, and AC impedance values were sequentially measured for each specimen one hour after current cut-off. After the electrochemical measurements were made, the specimens were removed from the tanks, and ultrasonic testing was conducted.

To perform ultrasonic testing, five spots on the concrete surface along the direction of the rebar were marked as shown in Figure 4. The direct pitch-catch A-scan method was used to obtain the UT signals at five spots for every cycle. Since the UT signals could be different at every point, the initial amplitude corresponding to each measured point was recorded before the specimen was connected to the DC power supply. As the accelerated corrosion experiment continued, the amplitude decayed as the corrosion of the rebars caused some deterioration in the concrete. The relative amplitude attenuation could be defined as the measured amplitude divided by the initial amplitude. In comparison with the electrochemical parameters that represent the global corrosion information, the average amplitude attenuation was calculated by taking the average of the amplitude attenuation at five spots. In this study, the deterioration of the RC members was mainly induced by corrosion; therefore, the amplitude attenuation only reflected the corrosion damage. The UT amplitude attenuation could significantly trace the deterioration along the path of the ultrasonic wave; however, the type of deterioration could not be distinguished. Therefore, an engineering judgment or other measurements should be conducted to complete the diagnostics.

TABLE 2
The concrete mix designs.

		Mix Proportion (Kg/m^3)				
Label	W/C	Water	Cement	Sand	Aggregate	SP*
Group A	0.35	213.5	610.2	494	1010.8	6.1
Group B	0.4	213.5	533.9	565.4	1010.8	5.34

*SP is F-type superplasticizier.

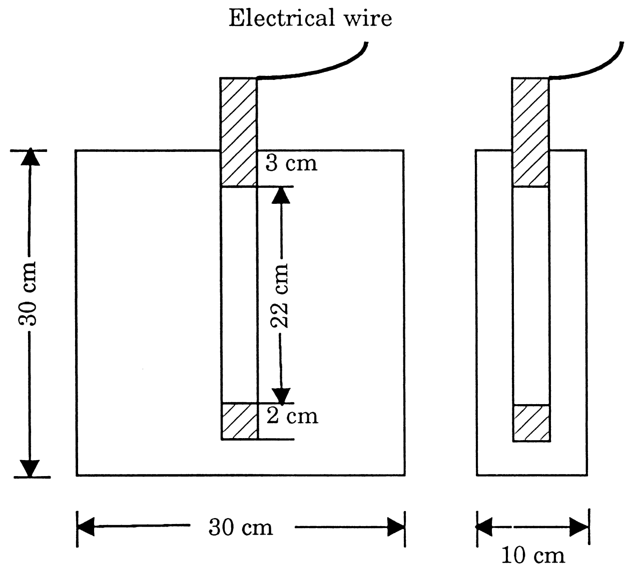

FIG. 3.
Illustration of the specimens.

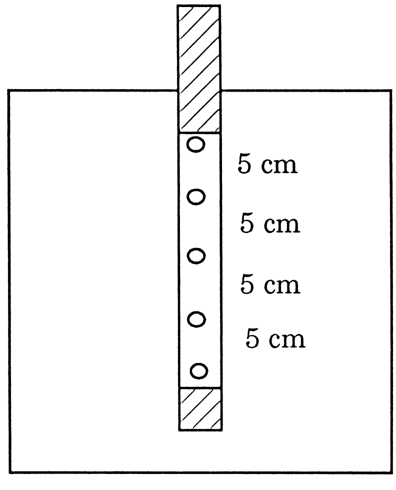

FIG. 4.
UT measuring locations.

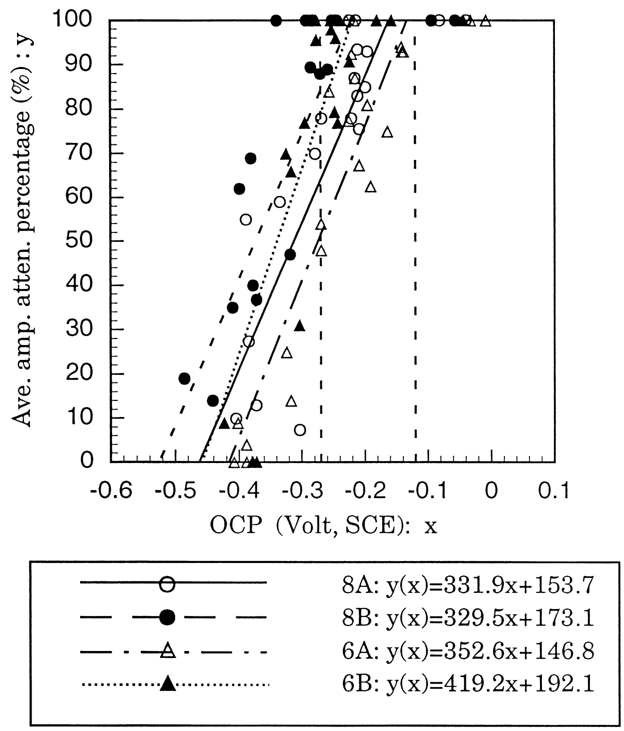

FIG. 5.
OCP values vs. average amplitude attenuation percentages.

Results and Discussions

OCP Values vs. the Average UT Amplitude Attenuation

OCP values represent the thermodynamic trend of corrosion. It is suggested by ASTM C876–91 (14) that the corrosion probability is less than 10% when the OCP value is higher than −200 mV Cu/$CuSO_4$ (−120 mV, SCE), and higher than 90% when the OCP value is lower than −350 mV Cu/$CuSO_4$ (−270 mV, SCE). The OCP values vs. the average UT amplitude attenuation percentages for each group are illustrated in Figure 5. Two vertical dashed lines in this figure represent two OCP margins according to ASTM C876–91.

It is shown in Figure 5 that the OCP values and the average amplitude attenuation percentages fit fairly well the linear relationship for each group. Linear regression was constructed for data whose average amplitude attenuation percentage was not 0 or 100. It can be found that the UT amplitude for group A began to decay at a nobler OCP value than did that for group B with the same rebar size. Also, it can be found that for specimens with the same water-cement ratios, the corresponding amplitude attenuation for specimens with #6 rebars was more serious than was that for those with #8 rebars when the same OCP value was observed at the beginning stage (amplitude attenuation percentage from 50–100%). To explain this phenomenon, we need to consider the ultrasonic wave path shown in Figure 6. Since the diameter of the UT probes was 2 cm, the direct path for the ultrasonic wave for

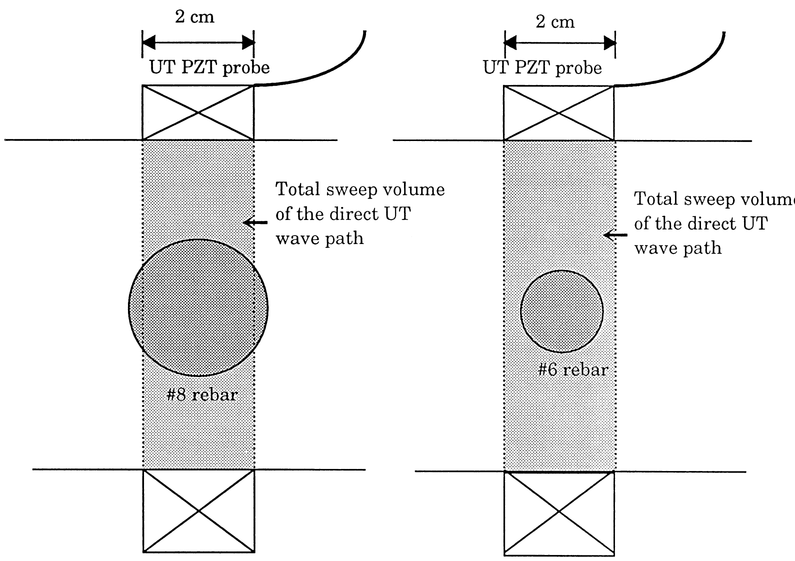

FIG. 6.
Illustration of the rebar size effect on UT amplitude attenuation.

specimens with #6 rebars swept a larger concrete volume than did that for the specimens with #8 rebars. It appears that the ultrasonic wave attenuation for detectable concrete deterioration due to corrosion was more significant for specimens with smaller rebar. As the corrosion process continued, the microcracks interconnected and formed major cracks such that the rebar-size effect became negligible. Therefore, the above-mentioned trend disappeared at the later corrosion stage because the path and size of the major cracks dominated the amplitude attenuation.

OCP values only can provide information for corrosion probability and cannot indicate what the corrosion probability is when the OCP value is within −120 mV (SCE) and −270 mV (SCE). On the other hand, the UT amplitude attenuation effectively reflected the corrosion damage. It is certain that there existed some degree of deterioration in concrete when the UT amplitude began to decay, no matter of what type the deterioration was.

Corrosion Rates vs. the Average UT Amplitude Attenuation

For either the DC linear polarization method or the AC impedance method, the polarization resistance, R_P (ohm·cm^2), can be measured. The corrosion current density, i_{corr} (Amp/cm^2), can be expressed as

$$i_{corr} = \left[\frac{\beta_a\beta_b}{2.303(\beta_a + \beta_b)}\right] = B \times \frac{1}{R_P} \tag{1}$$

This formula is called the Stern-Geary equation (15). β_a and β_b represent the Tafel's slopes of the anodic polarization curve and the cathodic polarization curve, respectively. The value of B is often taken as 26 mV (16) for steels in an alkaline environment (the pH value for a concrete environment is above 12.8).

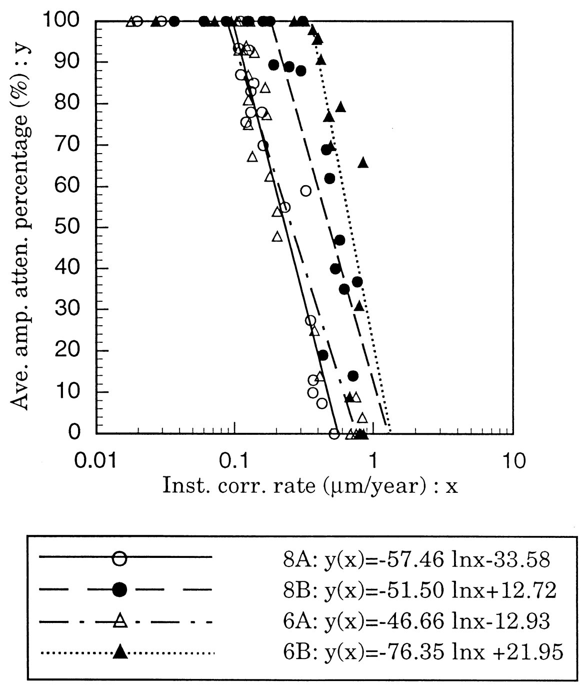

FIG. 7.
The instantaneous corrosion rates (DC linear polarization method) vs. average amplitude attenuation percentages.

After the corrosion current density is obtained, the instantaneous corrosion rate can be calculated from Faraday's law as

$$\Gamma_{corr} = \frac{i_{corr}}{nF} \times \frac{W_{Fe}}{D_{Fe}} \tag{2}$$

In the above equation, γ_{corr} (cm/sec) represents the thickness loss of the steel per unit of time; corrosion engineers sometimes choose mpy (mils per year) or μm/yr as the unit of γ_{corr}. F is the Faraday's constant, which is 96500 Coulomb/mole, and n is the valence of oxidant for the following oxidation reaction:

$$Fe \rightarrow Fe^{2+} + 2e^{-} \tag{3}$$

Thus, n is equal to 2. W_{Fe} (55.8 g/mole) is the atomic weight of the iron, and D_{Fe} (7.86 g/cm^3) is the density of the iron.

The instantaneous corrosion rates vs. the average UT amplitude attenuation percentages from the DC linear polarization method and the AC impedance method are plotted in Figures 7 and 8, respectively. Note that the semi-logarithm scale is selected because the instantaneous corrosion rate and the average amplitude attenuation maintain a linear relationship in this scale. As mentioned in the previous paragraph, the linear regression is conducted using the amplitude attenuation percentages between 0 and 100.

It can be seen that UT amplitude attenuation is easier to detect for lower water-cement ratio

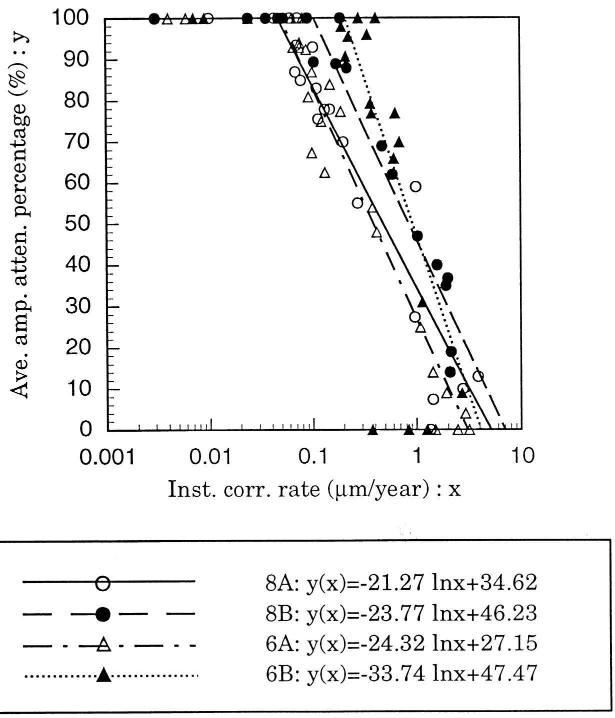

FIG. 8.
The instantaneous corrosion rates (AC impedance method) vs. average amplitude attenuation percentages.

specimens. The lower water-cement ratio specimens had denser microstructures, such that microcracks were easier to initiate and extend due to the smaller stress relief effect from the nearby micropores. This reflects the phenomenon of higher-strength concrete being more brittle. However, the rebars in the higher-strength concrete were more difficult to corrode because the time-span needed to obtain the same corrosion parameters for the higher-strength concrete was always longer than that of the lower- strength concrete. Although the difference was only one or two days for the accelerated corrosion experiments we performed, this corresponds to possibly several years for the natural corrosion process. Therefore, denser microstructures may keep corrosion media (e.g., chloride ions) from approaching rebars. Once the microcracks were initiated by corrosion, they extended faster because of the more brittle material property. From the figures, it appears that the decaying rate of the average UT amplitude with respect to the instantaneous corrosion rate is larger when the instantaneous corrosion rate is smaller. At the beginning stage, microcracks initiate and propagate due to corrosion products; however, after a major crack is formed, further corrosion only makes the major crack extend and open. Therefore, UT amplitude attenuation becomes more significant for lower instantaneous corrosion rate due to the large amount of the energy dissipated by microcracks. UT amplitude attenuation becomes smaller under higher instantaneous corrosion rates after major cracks form and propagate because the sizes and the paths of the major cracks dominate the energy dissipation, and not many microcracks can be initiated after the appearance of major cracks.

By comparing the figures, we can find that for the same UT amplitude attenuation percentage, the instantaneous corrosion rate obtained using the DC linear polarization method was lower than that obtained using the AC impedance method. This is because when the IR drop effect is not taken into account in the DC method, as shown in this research, it leads us to overestimate the polarization resistance (17) for rebars embedded in concrete. Consequently, the DC method will underestimate the instantaneous corrosion rate for rebars in concrete using Eqs. 1 and 2 when IR drop effect is not taken into account. The AC impedance method can, theoretically, separate polarization resistance from total resistance using the Nyquist plot (17) technique; therefore, no IR drop effect needs to be considered.

Thickness Loss vs. the Average UT Amplitude Attenuation

The thickness loss can be obtained by integrating the area of the instantaneous corrosion rate vs. the time curve. That means the thickness loss, s, is expressed as

$$s(t) = \int_0^t \Gamma_{corr}(t)dt \tag{4}$$

From the definition of the instantaneous corrosion rate, it is easy to find that the loss of thickness is a function of time and that it represents the average thickness loss of iron at a specific time. The reason for using the thickness loss as a corrosion parameter is explained as follows. During the corrosion process, the corrosion product itself will become a potential barrier such that the corrosion rate will slow down due to this potential barrier and the consumption of the readily accessible oxygen, and the corrosion open circuit potential will become nobler. Therefore, neither the instantaneous corrosion rate nor the open circuit potential is an increasing function with respect to time. However, the loss of thickness is an increasing function with respect to time because it is defined by integrating the area of the instantaneous corrosion rate vs. the time curve, and the instantaneous corrosion rate will never be negative due to the nature of corrosion. If one makes a judgment about whether or not the rebar is corroded based on the instantaneous corrosion rate or open circuit potential, an inaccurate conclusion may be drawn. It was suggested (16) that one should use the long-term trend of the instantaneous corrosion rate and OCP values to make a judgment. A record of the electrochemical measurements is necessary. It seems that the thickness loss can help us make a decision according to the current value; however, while the thickness loss is obtained from the record of the corrosion rate measurements, the current thickness loss actually needs time history of the corrosion rate. The thickness loss vs. the average amplitude attenuation percentages is illustrated in Figures 9 and 10 for the DC linear polarization method and AC impedance method, respectively.

Figures 9 and 10 show that the thickness loss and average amplitude attenuation have a nonlinear relationship. It appears that the UT amplitude for the lower water-cement ratio groups began to decay at smaller thicknesses loss than did the higher water-cement ratio groups. This again verifies that a more brittle matrix cannot suffer stress from swelling corrosion products; in this case, microcracks will initiate and extend.

It is also found that the slope for the nonlinear relationship between the thickness loss and the amplitude attenuation percentage of group A is more negative than that of group B. As

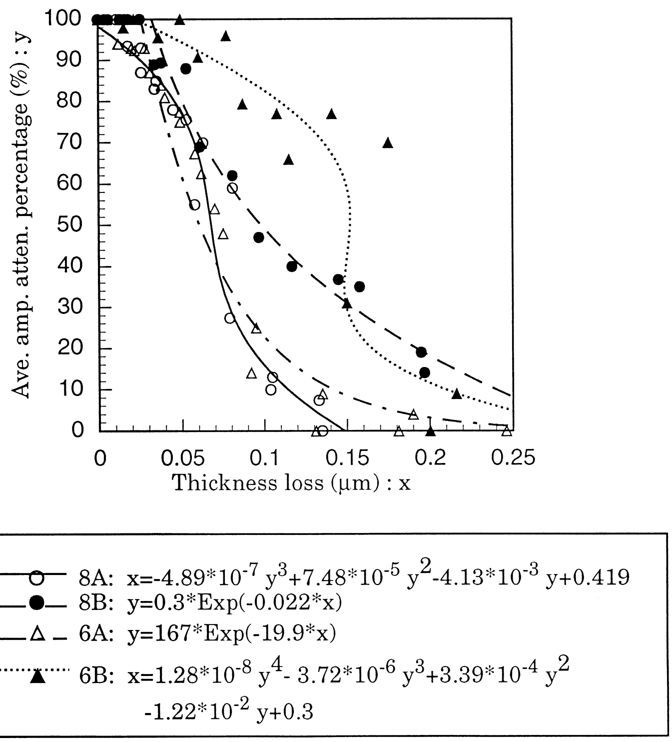

FIG. 9.

The thickness loss (DC linear polarization method) vs. average amplitude attenuation percentages.

the thickness loss increased, the stresses induced by the corrosion products resulted in further deterioration in the brittle material.

General Discussion

The electrochemical parameters were found to have interesting relationships with the average UT amplitude attenuation in the experiments. Extension of the A-scan method, which was used in this study, to the C-scan method could possibly be done because the C-scan method only accumulates results from the A-scan method point by point. However, we must remember that the initial UT amplitude may be different point by point; a careful consideration of different initial UT amplitudes point by point should be completed first to generate equal amplitude attenuation contours in the C-scan. Although we have not proved that this method can be successfully used for detection of local corrosion damage, we consider this study to be a pioneer work, with further research needing to be done.

Because the UT method is based on mechanical wave propagation, it would be interesting to know how the UT amplitude attenuation signals are related with mechanical deterioration in RC members. If such a relationship can be found, the UT amplitude attenuation method will be more effective than other electrochemical methods.

Although we conclude that the UT amplitude attenuation method is an alternative nonde-

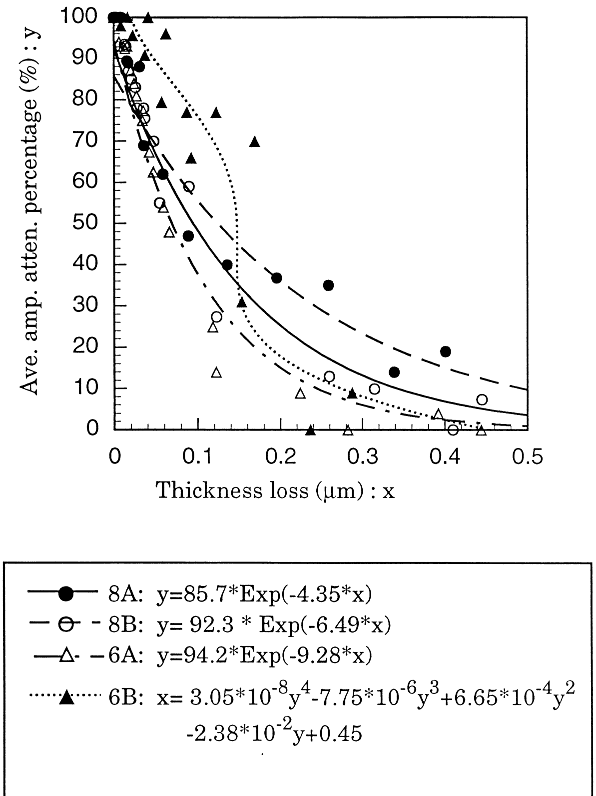

FIG. 10.
The thickness loss (AC impedance method) vs. average amplitude attenuation percentages.

structive method, it has been found that UT amplitude attenuation depends on the material properties (e.g., water-cement ratio) and rebar size. A series of studies to determine the relationship between UT amplitude attenuation and the water-cement ratio (or compressive strength of concrete) and the relationship between UT amplitude attenuation and rebar size should be carried out.

Conclusions

The average UT amplitude attenuation percentages have been found to have interesting relationships with electrochemical parameters in accelerated corrosion experiments. The average UT amplitude attenuation in the higher strength concrete was easier to detect because of the brittle microstructure. Due to the rebar size effect, specimens with smaller size rebars had more significant UT amplitude attenuation than those with larger size rebars in the beginning stage of corrosion process.

This paper has provided another possible method for evaluating corrosion damage. Although the proposed approach is not as mature as traditional electrochemical methods, it appears that this method is a fruitful area for further research.

Acknowledgment

The authors want to express their thanks to the financial support from NSC under the contract NSC 86-2211-E-019-007.

References

1. A. Macias and C. Andrade, Bri. Corr. J. 18, 82 (1983).
2. R. Francois, G. Arliguie, and D. Bardy, Cem. Concr. Res. 24, 401 (1994).
3. W.N. Reynolds and R.L. Smith, J. of Physics D: App. Phy. 17, 109 (1984).
4. V.L. Siviryuk and I.V. Gramotnik, Defektoskopiya 1, 60–62 (January 1991).
5. Y.V. Zakharov, V.V. Grebennikov, M.V. Grigor'ev, and Y.S. Glek, Energomashinostroenie 1, 22 (1984).
6. S. Perring, R.L. Smith, B. Hudson, and W.N. Reynolds, Phil. Mag. A 52, 721 (1985).
7. R.E. Green Jr. and J.C. Duke Jr., Int. Adv. in NDT 6, 125 (1979).
8. O. Buck, W.L. Morris and M.R. James, J. of Nondestructive Eva. 1, 3 (1980).
9. E.P. Papadakis, K.A. Fowler and L.C. Lynnworth, J. of the Acou. Soc. of America 53, 1336 (1973).
10. J. Krautkrämer and H. Krautkrämer, Ultrasonic Testing of Materials, 4th edition, Springer-Verlag, Berlin, 1990.
11. H.W. Chang and K.S. Law, Con. Int., 42 (October 1983).
12. V.R. Sturrup, F.J. Vecchion and H. Caration, ACI SP-82, 201 (1984).
13. J.R. Leslie and W.J. Cheesman, J. of ACI 46, 17, (1949).
14. ASTM C876–91, Standard Test Method for Half-Cell Potentials of Uncoated Reinforcing Steel in Concrete, ASTM, Philadelphia, 1991.
15. M. Stern and A.L. Geary, J. of the Electrochemical Soc. 104, 56 (1957).
16. R.K. Dhir, M.R. Jones, and M.J. Macarthy, Cem. Concr. Res. 23, 1443 (1993).
17. R. Huang, W.D. Yeih, J.J. Chang, and C.C. Yang, J. of Marine Sci. and Tech. 2, 53, (1994).